



ELSEVIER

Peptides 22 (2001) 979–994

PEPTIDES

## N-Acetylcarnosine, a natural histidine-containing dipeptide, as a potent ophthalmic drug in treatment of human cataracts

Mark A. Babizhayev<sup>a,b,\*</sup>, Anatoly I. Deyev<sup>a</sup>, Valentina N. Yermakova<sup>b</sup>, Yuri A. Semiletov<sup>a</sup>, Nina G. Davydova<sup>b</sup>, Natalya I. Kuryshcheva<sup>b</sup>, Alexander V. Zhukotskii<sup>a</sup>, Ita M. Goldman<sup>a</sup>

<sup>a</sup>Innovative Vision Products, Inc., County of New Castle, DE 19810, USA

<sup>b</sup>Moscow Helmholtz Research Institute of Eye Diseases, Russian Federation, Russia

Received 22 July 1999; accepted 22 December 2000

### Abstract

A study was designed to document and quantify the changes in lens clarity over 6 and 24 months in 2 groups of 49 volunteers (76 eyes) with an average age of  $65.3 \pm 7.0$  enrolled at the time of diagnosis of senile cataracts of minimal to advanced opacification.

The patients received N-acetylcarnosine, 1% sol (NAC) (26 patients, 41 eyes = Group II), placebo composition (13 patients, 21 eyes) topically (two drops, twice daily) to the conjunctival sac, or were untreated (10 patients, 14 eyes); the placebo and untreated groups were combined into the control (reference) Group I. Patients were evaluated upon entry, at 2-month (Trial 1) and 6-month (Trial 2)-intervals for best corrected visual acuity (b/c VA), by ophthalmoscopy and the original techniques of glare test (for Trial 1), stereocinematographic slit-image and retro-illumination photography with subsequent scanning of the lens. The computerized interactive digital analysis of obtained images displayed the light scattering/absorbing centers of the lens into 2-D and 3-D scales.

The intra-reader reproducibility of measuring techniques for cataractous changes was good, with the overall average of correlation coefficients for the image analytical data 0.830 and the glare test readings 0.998. Compared with the baseline examination, over 6 months 41.5% of the eyes treated with NAC presented a significant improvement of the gross transmissivity degree of lenses computed from the images, 90.0% of the eyes showed a gradual improvement in b/c VA to 7–100% and 88.9% of the eyes ranged a 27–100% improvement in glare sensitivity. Topographic studies demonstrated less density and corresponding areas of opacification in posterior subcapsular and cortical morphological regions of the lens consistent with VA up to 0.3. The total study period over 24 months revealed that the beneficial effect of NAC is sustainable. No cases resulted in a worsening of VA and image analytical readings of lenses in the NAC-treated group of patients. In most of the patients drug tolerance was good. Group I of patients demonstrated the variability in the densitometric readings of the lens cloudings, negative advance in glare sensitivity over 6 months and gradual deterioration of VA and gross transmissivity of lenses over 24 months compared with the baseline and 6-month follow-up examinations. Statistical analysis revealed the significant differences over 6 and 24 months in cumulative positive changes of overall characteristics of cataracts in the NAC-treated Group II from the control Group I.

The N-acetylated form of natural dipeptide L-carnosine appears to be suitable and physiologically acceptable for nonsurgical treatment for senile cataracts. © 2001 Elsevier Science Inc. All rights reserved.

**Keywords:** Antioxidant; Natural product dipeptide; N-acetylcarnosine; L-carnosine; Ophthalmic drug; Lens; Cataract; Ocular administration

### 1. Introduction

Cataract is the leading cause of blindness worldwide, accounting for over 50% of the world's blind population,

affecting some 17 million people [36]. Although surgical extraction of the involved lens is effective, there is a considerable interest in identifying the risk and protective factors involved in cataractogenesis [35]. Age-related cataract is a multifactorial disease, and different risk factors appear to play a role for different cataract types. Numerous studies postulate that oxidative stress to the lens mediated by reactive oxygen species and lipid peroxides produced in the crystalline lens can initiate the process of cataractogenesis [2,13,18,22,23,31,34]. It is established that superoxide an-

\* Corresponding author. Tel.: +7-095-977-2387; fax: +7-095-977-2387.

<sup>1</sup> Present address: Ivanovskaya 20, Suite 74, Moscow 127434, Russian Federation.

E-mail address: markbabizhayev@mail.ru (M.A. Babizhayev).

ion radical, hydroxyl radical, hydrogen peroxide, singlet oxygen and lipid peroxides can be generated by photochemical reactions in the lens surroundings triggering the development of different forms of cataract [7,11,30,33,38] and that the use of antioxidant supplements appears to be protective against cataract [29]. Peroxide damage to the lens plasma membranes may lead to disturbance of their permeability for ions, loss of thiol groups of the membrane-bound crystallins and the appearance of new fluorophores and also large protein aggregates with low solubility (scattering matrix) in the substance of the lens thus affecting the development of cortical (C), posterior subcapsular (PSC) and nuclear (N) cataracts [4,10,11,20].

L-Carnosine ( $\beta$ -alanyl-L-histidine) and related  $\beta$ -alanyl histidyl dipeptides (anserine and balenine) are generally found in mM concentrations in several mammalian tissues, potentially exhibiting different metabolic activities [14]. The previously published data suggest that L-carnosine has excellent potential to act as a natural antioxidant with hydroxyl radical, singlet oxygen scavenging and lipid peroxidase activities [14,21]. A striking effect of L-carnosine is its demonstrated ability to prevent, or partially reverse, lens cataract [3,19]. Exogenous carnosine entering the organism intravenously, intraperitoneally, with food or topically to the eye, is not accumulated by the tissues but is excreted in the urine or destroyed by carnosinase, a dipeptidase enzyme that is present in blood plasma, liver, kidney and other tissues except muscle and probably lens [3,24].

The N-acetyl derivatives of histidine, carnosine and anserine exist in the cardiac and skeletal mammalian muscles and the total concentration of these imidazoles may lie within the measured range of L-carnosine in skeletal muscle ( $\sim 10$  mM) [27]. The pharmaceutical compositions containing N-acetylcarnosine aluminum salt have been reported for the treatment of gastric ulcers [28]. Among 29 dipeptides of the carnosine family tested as potential substrates for a highly purified human serum carnosinase preparation, N-acetylcarnosine and few other compounds were not hydrolyzed, [24] thus promising a prolongation of physiological responses to the therapeutic treatments. A knowledge of corneal and iris/ciliary body esterase activity, in particular, acetyl esterase (EC 3.1.1.6) and, in addition to esterase, the identified N-acetyltransferase activities [1] prompted the development of a prodrug of L-carnosine in its ophthalmic application as antioxidant such as the chemically characterized N-acetylated form of the dipeptide [16]. Experiments with N-acetylcarnosine (NAC) (1% sol) topically administered to the rabbit eyes (instillation, subconjunctival injection, ultrasound-induced administration) revealed its penetration into the eye and accumulation of the native form of L-carnosine in aqueous humor within 15–30 min of administration extending in order of the indicated therapeutic modalities [6,8,16]. The NAC molecule showed a moderate inhibiting activity for catalysis of phosphatidylcholine liposomal peroxidation *in vitro*, less pronounced than that of L-carnosine [16].

The advantage of NAC to act as an *in vivo* universal antioxidant with physiological and therapeutic relevance deals with its ability to give efficient protection against oxidative stress in the lipid phase of biological membranes and in aqueous environment due to turnover into L-carnosine [6,8,16]. Due to relative hydrophobicity compared with L-carnosine, NAC might penetrate through the cornea gradually, thus maintaining longer the active therapeutic concentration of L-carnosine in aqueous humor of the treated eye [16]. Different techniques of ocular administration of NAC showed its excellent tolerability to the eye, safety and the lack of possible side effects [16]. The clinical study was designed to be a prospective evaluation of the lens opacities and visual function in cataractous patients who applied topically to the eye (eye drops) the physiologically acceptable solution of NAC [6,8].

## 2. Subjects and methods

### 2.1. Clinical design

The research was performed in agreement with the principles of Helsinki Declaration (ed. 1964 and following revisions) and the "Guidelines on the quality, safety and efficacy of pharmaceutical products used in European Community" (91/507/CEE). Each patient received verbal and written explanations about the object of the trial and the properties of the drugs which he would take. Each patient was also informed about his rights, particularly the right of withdrawing from the trial without any justification, and informed consent to the trial was obtained. All the patients were computer randomized concurrently in two clinical groups as to NAC-treated or placebo-treated cases and controls (Table 1) upon the entry in the study. The number of patients needed for each trial was chosen in order that the patient groups were well matched, with no significant differences in demographic and clinical characteristics. The sample size calculations depended on the accuracy of the monitoring method employed for any of the major types of cataract assessed.

A total of 49 elderly patients (76 eyes) completed the 6-month and the 2-year protocol. They were divided into following groups: I, control group representing untreated (10 patients, 14 eyes) or treated with placebo compositions (13 patients, 21 eyes); II, taking the composition of drops containing NAC (26 patients, 41 eyes), (Table 1). Twenty patients (34 eyes) with cataracts were enrolled into the study from the Consulting Division of Moscow Helmholtz Research Institute for Eye Diseases and follow-up examinations carried out every 2 months within a 6-month period (Trial 1). Twenty nine elderly patients with cataracts (42 eyes), supervised by the same observer, were enrolled from the Ophthalmic Division of Innovative Vision Products Inc. with ophthalmic examinations carried out every 6 months

Table 1  
Population characteristics of patients

Parameter	Group I, control	Group II, treated with instillations of NAC, 1% sol
<i>Trial 1</i> (Baseline study: 2 visits; Follow-up period: 6 months, 3 visits)		
No. (total)	10	10
No. eyes	16	18
Males	5	5
Females	5	5
Age-mean (years $\pm$ SD)	67.1 $\pm$ 7.1	67.0 $\pm$ 4.1
Epidemiologic status (N <sup>o</sup> eyes)	S (13); S <sub>compl</sub> (3)	S (16); preS (2)
<i>Trial 2</i> (Baseline study: 1 visit; Follow-up period: 24 months, 4 visits)		
No. (total)	13	16
No. eyes	19	23
Males	7	8
Females	6	8
Age-mean (years $\pm$ SD)	64.3 $\pm$ 6.7	64.0 $\pm$ 8.5
Epidemiologic status (N <sup>o</sup> eyes)	S (18); S <sub>compl</sub> (1)	S (19); S <sub>compl</sub> (4)

for 2 years (Trial 2). Neither the investigators nor the patients knew who was taking NAC.

The population characteristics are shown in Table 1. The groups were compared for sex composition, mean age of patients, severity of initial symptoms and presence of concomitant diseases: none of the baseline differences between the different groups was significant. The study did not measure or evaluate the use of other topical or nutritional antioxidant between the two groups. The control group and the treated group did not take any prescribed antioxidant vitamins that might have added to the antioxidant level. The two studied groups were similar in smoking history, as well as sunlight exposure and alcohol use. There was no any substantial difference in the use of sunglasses between the two studied groups. There was no difference where the patients lived, or occupational hazard exposure between the two examined groups.

## 2.2. Patient study

The examined eyes had cortical, nuclear, posterior subcapsular, or mixed lens opacities and varying degrees of nuclear color or brunescence. The patients had minimal to advanced lens cataractous changes. Eligibility criteria included a confirmed diagnosis of senile (S) cataract according to the medical history of disease, clinical observations and epidemiological study. Each patient met the following inclusion criteria: (1) availability for study of both lenses in each patient; (2) the presence of a cataract in at least one eye; (3) the cataracts were judged not to require surgery in the near future (2 years) based on the patients' visual needs and ocular symptomatology; (4) 52 to 80 yrs of age; (5) pupillary dilation could be done safely. Patients were not included if they had any other ocular disease such as glaucoma or clinically significant diabetic retinopathy, previous laser retinal photocoagulation, prior corneal or anterior seg-

ment surgery or corneal scars which would interfere with visualization or photography of the anterior segment, or mature cataract (VA less than 0.1) in both eyes, and would likely be candidates for cataract surgery within 1 year. Excluded were monocular aphakics and patients with secondary cataracts (e.g., cataracts associated with steroid intake, total body or local irradiation, local inflammatory or degenerative process and ocular trauma). Patients with known or presumed hypersensitivity to any component of the ophthalmic medications (active substances or excipients), or patients treated with drugs which could interfere with this trial were also excluded from the study together with the subjects wearing contact lenses or suffering from concomitant ocular diseases.

## 2.3. Topographic and 3-D visualization of human cataracts

The recently developed technique of lens photography and cataract grading and measurement permits an adequate assessment of cataracts in human longitudinal studies [15]. The clinical standardization system uses the serial images obtained by the stereocinematographic slit-image and retroillumination photography with the regular slit-lamp camera consecutively focused on the lens objects to overcome the problem of stereoscopy and depth of field. This system gives a topographic and 3-D volume visualization for nuclear, cortical and posterior subcapsular opacities in human cataracts supplemented with digital image analysis and 3-D computer graphics. The important image contents are discriminated from the serial negatives supplied with a standard density reference and the rigorous computer-based image processing digitally enhances the contrast of lens opacity features and structures the 3-D composite of the lens revealed from the optical scanning tomographic study of the anterior eye segment [26]. The measuring characteristics of

different types of cataract include the average lens area degree of clouding (M) computed from the retro-illumination images [12,17]. The light transparency histograms (H) represent the distribution of grey values in different layers of the cataractous lens captured optically in contrast and electronically displayed from the subsequent slit-lamp images of cataract [17]. Mean values of H correspond to the intensity of lens cloudings, whereas the SE values represent heterogeneities of opacities throughout the lens layers. The intra-reader reproducibility for image analytical characteristics derived from the stereocinematographic slit-image and retro-illumination photographs was good with the overall average of correlation coefficients 0.911 and high between observer kappa scores [15]. The method reduces the cost and complexity of epidemiological study of age-related cataract, including clinical trials of anticataract medications by reducing the number of participants while at the same time increasing the power of the study.

#### 2.4. Evaluation techniques

The evaluation system used to diagnose and graduate the severity of lens opacities performed at each visit of a patient included (1) interviewing on patient's medical history; (2) measurement of best corrected (b/c) visual acuity (VA); (3) direct and indirect ophthalmoscopy; (4) glare test with optimal correction (for Trial 1); (5) stereocinematographic Zeiss photo-slitlamp examination and photography; (6) consecutive Zeiss photo-slitlamp retro-illumination photography: anteriorly focused and posteriorly focused; (7) quantitative interactive digital image analysis of obtained images from (5) and (6) with 3-D computer graphics; (8) clinical lens grading after maximum permitted mydriasis. All findings were recorded with drawings on standard documentation sheets.

#### 2.5. Lens slit-lamp photography

All patients underwent standardized slit and retro-illumination lens photography on the Zeiss 30 SL photo-slit-lamp with the pupil maximally dilated. For this a narrow slit was imaged in the transparent system of the anterior ocular media in such a way that the observation and illumination axes formed as large an angle as possible and the ocular fundus remained dark. The slit beam was 0.3 mm wide  $\times$  9 mm long angled at 30° to the visual axis; the same image scale (magnification) of  $\times$ 1.0 or 1.8 was selected in each set of photographs. For the retro-illumination photography either a broad, vertical beam was directed centrally through the dilated pupil at one side, or a narrow vertical beam, directed at a small angle (5°) to the central axis of the dilated pupil was used and the passage area of the illumination bundle was as far as possible from the object in the lens to be observed. Two photographs were taken with the slit beam on each side of the pupil during retro-illumination photography to allow the flash reflex [25]. The flash reflex

could be eliminated later using the interactive measuring program. The flash intensity was set at 5, equivalent to 200 watt seconds (W-sec). Efforts were made in this study to reduce any variation in the photographs by using the same camera, the same film from the same batch, and using only one photographer. Furthermore, aperture setting and shutter speed was the same for all photographs. In all cases, film was developed using identical procedures. The opacities were recorded in focal illumination and the low depth of field made the surroundings appear unfocused. The neutral density step reference wedge was captured in the plane of focus of the camera at each negative film to calibrate the illumination of the slit aperture. This recording also took into account the non-linear logarithmic nature of film response. Serial black/white photos were taken during two-to-three subsequent settings of the focal plane of the optical section that made it possible to discriminate in contrast every optical feature of anterior segment of the eye from cornea to posterior lens capsule on at least one of the slit-lamp images (stereocinematographic principle). During the slitlamp examination the clinician made sure that only the important image contents were shown and all other unimportant details and sources of disturbance such as reflections, were eliminated. This precise "interactive" role of the operator was realized also upon the consecutive digital image analysis in computerized assembling of the composites of the crystalline lens.

#### 2.6. Grading methods

Lens changes were graded according to anatomical location, severity and coevaluated with the visual acuity. The two- to-three black/white slit images, two retro-illumination images and the reference were used to grade the type and severity of cortical, nuclear, posterior subcapsular cataract and nuclear density. The nucleus was examined with a thin ( $\sim$ 0.1 mm) slit beam of 8 to 9 mm in height set at an incident angle of reproducible slit orientation of 30°. The slit passed through the anatomic center of the lens (the embryonic nucleus) and the clarity of the optical section of the nucleus compared to the reference photograph of nuclear cataract and graded accordingly to the technique described by Taylor and West [32]. The densities of nuclear opacities as seen on clinical slit-lamp examination are graded in comparison with a set of standard photographs (Grades 0–4) with increasing nuclear opacity. In the presence of cortical opacities, which may cause intense light scatter, care was taken not to overcall the density of the nuclear opacity. In these cases, particular attention has been directed to the uniformity and distribution of the nuclear opacity. The reference photographs were 35 mm transparencies that are viewed in a hand-held, battery-operated slide viewer.

The cortex was examined using the reproducible optical plain setting in retro-illumination in terms of segments involved [32]. The slit-beam was relatively wide (0.5 to 1

mm) and short (4 to 5 mm) in height. It was angled through first one side of the pupil and then the other so that the entire cortex could be examined in clear retro-illumination. The focus of the slit-lamp was altered so that both the anterior and posterior cortical regions were each examined in clear focus. The presence or absence of cortical wedges, or spokes, or other cortical opacities was then assessed. Only cortical opacities that could be seen in retro-illumination were graded [32]. If cortical opacities were present, they were graded by estimating the proportion of the total circumference of the lens occupied by the combined cortical opacities as if they were adjacent. This was done by visually dividing the pupillary area first into quadrants and then into eighths. The circumferential extent of each opacity was assessed and then the combined circumference of all opacities estimated. Vacuoles were seen as discrete black rings with a clear center on retro-illumination. Cortical cataracts (Grade 0) had no opacities; grade 1 represented opacities which then combined occupied less than one eighth of circumference; grade 2 included opacities which when combined occupy less than one quarter of circumference; grade 3 presented opacities which when combined occupy less than half of circumference; grade 4 included opacities which when combined occupy more than half of circumference.

Posterior subcapsular opacities were also assessed by using retro-illumination and their overall vertical and horizontal dimensions measured using the calibration of the slit beam height. Both the vertical and horizontal dimensions were recorded. These dimensions were then multiplied together to give an approximation of extension.

Based on the VA, grade 0 was given for no opacification, grade 1 for early changes with no expected impact on VA, grade 2 for opacification consistent with VA of 0.6, grade 3 for opacification consistent with VA up to 0.2, and grade 4 for opacification consistent with VA lower than 0.2.

### 2.7. Quantitative assessment and image analysis

The opacities were digitized and the intensity values of individual image pixels were used for the numerical determination of their areas and densities. For technical realization of the image analytical procedures, the IBAS Interactive Image Analysis System (Zeiss, Germany) additionally equipped with Semi-Automatic Evaluation Unit, and Array Processor, Printer (OK1 DP-125) was used. A fully automatic measuring program provided valid measurements of the light intensities and densities in the lens image and comparisons with the step wedge image regardless of any change in flash output and also compensation for changes in development of the film which affects the density curve ( $\gamma$ ) of the negative. The film used for photography was Micrat 200 (Tasma, Kazan, Russia) monochrome film chosen because of its extended density range and fine grain. Negatives of the lens images were back-lit with the uniformly diffused source 'TL' 13W/33 (Philips, Germany) from a day-light

lamp when positioned on a look-up table and the anterior surface of the negative faced the camera. Images were captured by a RCA TV camera (USA) with a Plumbicon tube (625 lines interlaced, 25 frames/sec, short persistence time) which ensured a highly linear transfer function between light intensity and electrical signal, with a photoobjective SMC PENTAX Macro ( $\times 10$ ) (Japan). The degree of enlargement of the negatives was adjusted so that the image of the pupil became equal in diameter to a circle of set size on the TV screen.

The analytical measurements of retro-illumination photos and the serial subsequent slit-lamp images of the lens made adjustments for variations in background due to variation in a reflection from the fundus. The light intensities passed through the lens image elements ( $I_{ij}$ ) were automatically divided (normalized) by the background illumination intensity measured in the free image pixels ( $I_o$ ) to obtain a transmission index ( $I_{ij}/I_o$ ) or its logarithmic value [ $\lg(I_{ij}/I_o)$ ] and compose the matrix of density inhomogeneities in the 2-D scale. The lowest detectable density was set to correspond to that of the retro-illumination background in an area of the lens unaffected by cataract. Measurements were provided in each of the two captured retro-illumination photos used to subtract the corneal reflex by the software interactive filtering. The lens retro-illumination images were sectioned into up to several <<equidensities>> [12,17]. Individual transmittance values for each pixel were acquired in a calibrated linear scale, where 0 and 255 correspond to 100% (<<black>>) and 0% (<<white>>) transmittances, respectively. Each video frame was stored in real time on a memory according to the format matrix  $512 \times 512$  pixels. Final images were stored on disk after subtraction and equalization of the background due to optical and electronic noise. Software enabled to select an individual area of the cortical cataract as a measuring field which was calculated with the help of the circular mask selection, whose position was under the control of the analyzer and observer. The analytical measurements were carried out in the automatic order using the packages of the IBAS-2 programs and individual authorized supplementation DIAMORPH [17]. The data on grading the retro-illumination photos were expressed as the average area degree of clouding [12,17]  $\{M = (OD_{ij} \cdot A_{ij}) / (\sum_{ij}^L OD_{ij} \cdot A_{ij})\}$  with the standard deviation about the mean, where  $OD_{ij}$  and  $A_{ij}$  are the corresponding measured values of optical density and area for the raster pixels. The analytical plan performed for the different comparisons included the number of functions: standardization of the image input, including image averaging, shading correction, image filtering, contrast enhancement, copying of the image sections, suppression of unwanted features within the image, reading and writing of images on hard disk; calibration of the image features and identification of measurement data, editing of the light intensity distribution along a selected profile, discrimination of the image features chosen for analysis within different gray thresholds after the image was scanned electronically and the density at each

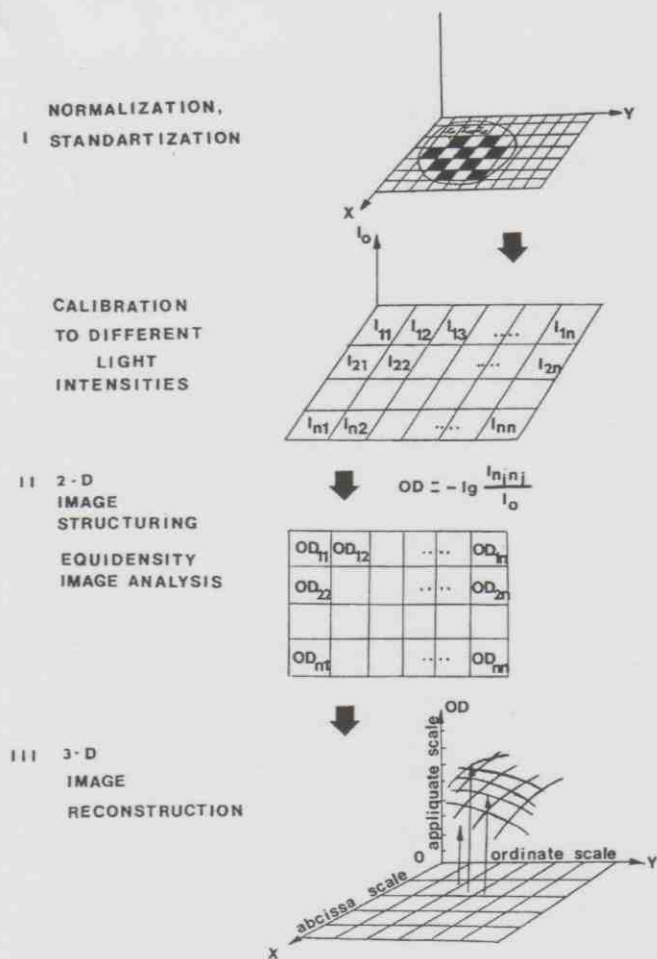


Fig. 1. Image analytical procedures provided with the aid of an automatic measuring program. Functions included 2-D structuring of an image, measurements of the surface density, specific area, mean linear dimension, curvature; determination of 3-D volume densitometric parameters and geometric transformation functions with data stored at each coordinate.

coordinate stored in the computer for further analytical procedures.

Using the serial subsequent slit-lamp images of the lens, 2-D and 3-D pictures of cataract were obtained [12,17]. The original lens image which included optical heterogeneities from images focused at various depths along optical sec-

tions was reconstructed in a 3-D scale and displayed from different angles of view (Fig. 1). The detailed structural parameters of the lens were rearranged from the light intensity measurements and included volume intensity, size, fractions of the opacity within the lens areas, average distance of their separation, density, difference between the normal or opacified lens units and their environment. Quantitative assessments of nuclear opacities and distribution of opacities (light transparency histograms) in adjacent morphological layers of the lens (H) were undertaken by determination of relative areas with different absorptive (transmittance) values based on the use of standard slitlamp photos with subsequent scanning and image processing. Posterior sub-capsular opacities were measured in retro-illumination and focal slit images using the discriminated area and density analysis.

### 2.8. Visual acuity

VA testing was performed to obtain the best distant VA with optical correction when required. VA was measured by projection screens (Carl Zeiss) with acuity lines in the following steps: 0.1 to 0.4 in 0.05 steps, 0.4 to 1.0 in 0.1 steps (Trial 1). The standard Snellen charts with a standard lighting were also used to monitor a Snellen VA (Trial 2).

### 2.9. Glare test

The contrast diminishing effect of glare is exaggerated in patients with opaque intraocular media, and VA is reduced. A method for measuring susceptibility to glare of a human vision system is schematically presented in Fig. 2. The examining room was dark (less than 20 ft candles) to assure maximum contrast of the projected target. Tests were performed with the best correction in place. The viewing distance was 300 mm for an acuity target and a single-dot glare light source of preselected intensity sufficient to generate glare in the vision system of a subject. The target was set in the same tangential plane at different gaps from the glare source. The target was represented as the self-luminous optotypes (figures or Landolt rings) displayed on the elec-

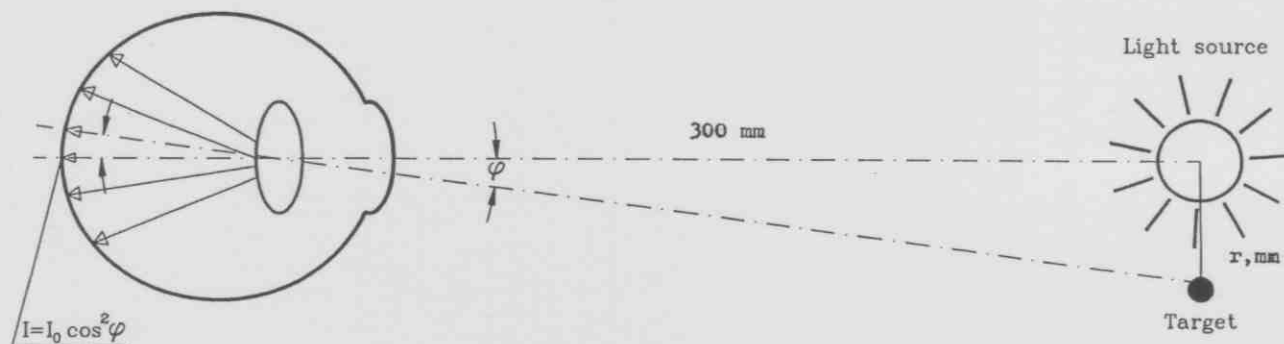


Fig. 2. Principle of glare test based on the measurements of glare radius ( $r$ , mm) as a reading of glare sensitivity.

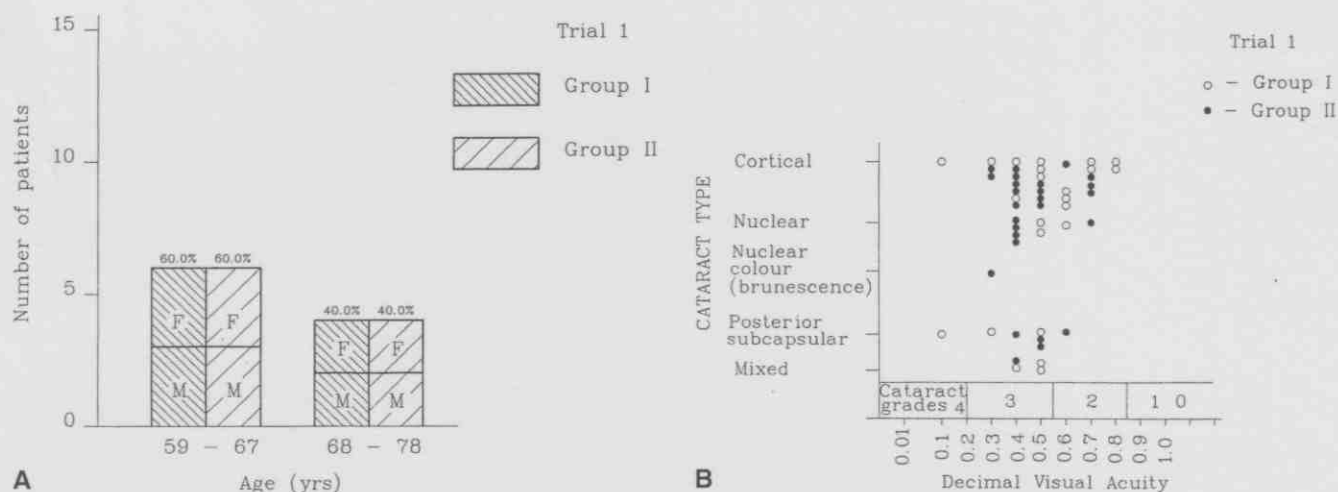


Fig. 3. (A) Age and sex distribution of patients with senile and age-related cataract in Trial 1. Elderly patients were enrolled in the control (reference) Group I ( $n = 10$ ) or treated with instillations of 1% N-acetylcarnosine—Group II ( $n = 10$ ) for 6 months. F = female; M = male. (B) Scattergraph of results outlining the distribution of cataract types, grades and best corrected decimal visual acuities of patients enrolled in Trial 1.

tronic table of  $5 \times 5$  mm with a light-sensitive diode or as the incandescent lamp-transilluminated optotypes of red or green color. The halo-meter technique is based on the measurements of a glare radius (defined as a target image projection for indicatrix of light scatter  $I = I_0 \cos^2 \varphi$ ) appeared when the glare source is activated, the patient is requested to cover the eye not being tested and asked to recognize the target (changing optotypes) during illumination of the eye with a glare source. The luminous target was shifted right and left upon the positioning to glare source and a patient was examined on the ability to name the optotypes. The resulting target-glare source distance measured (mm) in case a patient could just identify an optotype was assessed as a threshold measure of glare sensitivity in the tested eye. Because a patient cannot recognize an optotype-target when it enters the glare area ( $\ll$ halos $\gg$ ), the significant change of the glare radius value indicates the changes of intraocular light scattering (lens clarity). The significant increase and decrease of the glare radius to indicate worsening or improvement is usually a reading of 4 mm with a SE ( $n = 4$ )  $\pm 1$  mm that indicates changes in lens clarity towards opacification (increased light scattering) and clarification (decreased light scattering). The input of the light scatter wavelength was estimated using the colored (red or green) modes of the target. Data from the left and right eyes were analyzed separately.

#### 2.10. Treatments

The eye drops contained a 1% solution of NAC [6,8] in PBS showing good stability in aqueous solution. The eye drops were prescribed fresh prepared without additional preservation vehicle. The dosing schedule was to 2 drops instilled twice daily. The topical application of placebo (PBS-constituted) [6,8] (control Group I) had the same dosing schedule used for the active composition (Group II).

Trial 1 had a treatment period of 6 months and Trial 2 has a 2-year period of application.

#### 2.11. Statistical analyses

Statistical analysis was performed by Student's t-test;  $P = 0.05$  was taken as the upper limit of significance. To assess associations, correlation and linear regression analysis were used. For intra-operator correlation coefficient, the measurements from 2 visits (Trial 1, baseline) were considered as repeated measurements. The second photographs and glare test readings of the same patient by the same operator were taken at least 1 week apart from the first visit prior the treatment predication. The coefficient was computed by comparing the extra variation induced by repeated measurements of the individual operator with the existing variation between 20 patients. The clinical and photographic analyses related to image analytical procedures were additionally justified by statistical testing of mean values, variance, skewness, excess, distribution analysis (scatter diagram, linear and logarithmic distribution) as described earlier [17].

### 3. Results

The distribution of cataracts in the examined patients is shown in Figs. 3a, b and 4a, b. There was a good concordance in the severity of cataract between slit-lamp, photograding, glare test readings and the b/c VA results (Table 2). High values of the linear correlation coefficients ( $r$ ) for 34 examined eyes between VA and parameters of the glare test and image analytical grading ranged from  $-0.83$  to  $-0.52$  at initial study and from  $-0.80$  to  $-0.55$  at 5–6-months follow-up. Ophthalmic examinations indicated that the methodological variances of subjective and objective sys-

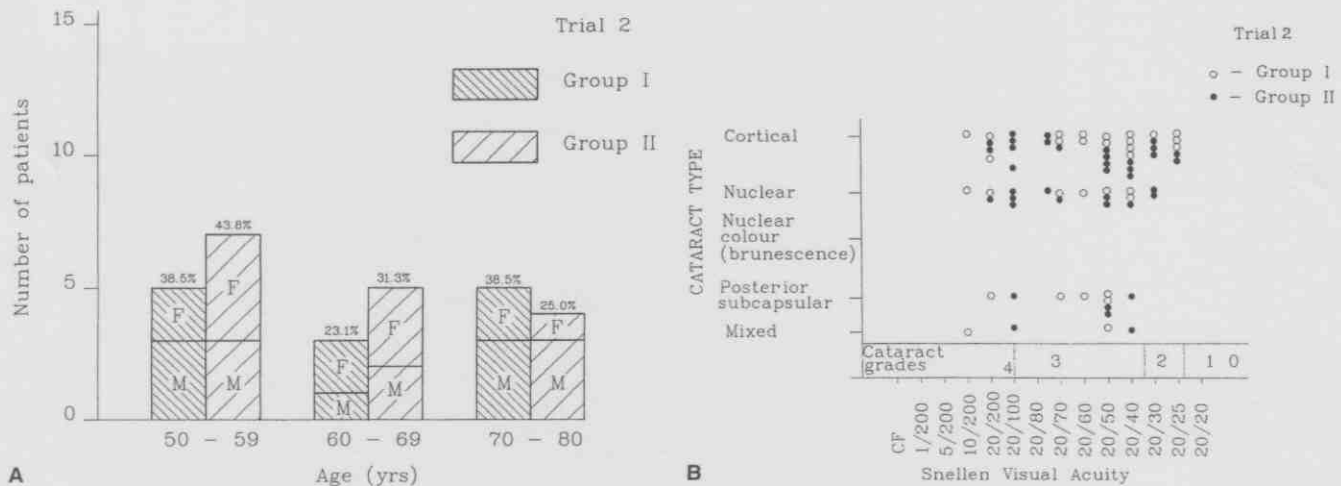


Fig. 4. (A) Age and sex distribution of patients with senile and age-related cataract in Trial 2. Elderly patients were enrolled in the control (reference) Group I ( $n = 13$ ) or treated with instillations of 1% N-acetylcarnosine—Group II ( $n = 16$ ) for 2 years. (B) Scattergraph of results outlining the distribution of cataract types, grades and best corrected Snellen visual acuities of patients enrolled in Trial 2.

tems of measurements were approximately equal. Most of the lens changes in the baseline examined cases were early and moderate (cortical, posterior subcapsular, mixed of grades 1 to 3) with the exception of cortico-nuclear mixed and nuclear color brunescence cataracts with more pronounced opacities (Figs. 3b and 4b).

Figs. 5a–e document a senile cataract with cortico-nuclear opacities (grade 4) used for further computerized editing and analysis of cataract. The individual areas in the optical section visualized in the photographs as the discontinuity zones selected with a slit were digitally made sharply visible during automatic analysis. During analysis of the presented retro-illumination images (Figs. 5c, d), the transition area influenced by flashlight is subtracted from quantification (equalized to the black background by suppression operation and image filtering functions).

Topographic structuring with image analysis of the selected equidensity lens areas and strict antero-posterior alignment of the lens layers were conducted to give a presentation of the whole lens affected by more than one type of opacity. 3-D structuring provided the geometric transformation with the data of the light intensity measurements stored at each coordinate and demonstrated the textures of the lens inhomogeneities in the axonometric image projection unidentifiable in the 2-D image analysis (Fig. 6). Pixel statistical analysis for individual lenses provided the gross quantitative degrees in the retro-illumination images and presented the spatial distribution of gray values in consecutive lens layers assembled from the digital optical sections (see M and H in the figures and text tables). Intra-operator correlation coefficient was obtained as repeated measurements for each combination of operator [1], eye

Table 2

Linear correlation coefficients (R)\* between the characteristics of cataractous patients measured by visual acuities, glare radius and photo slit-lamp image analysis at baseline and 6-months follow-up ophthalmic examinations (Trial 1)

Parameter	Baseline Study					5–6 Mos				
	VA	M	H	GR <sub>Red</sub> target	GR <sub>Green</sub> target	VA	M	H	GR <sub>Red</sub> target	GR <sub>Green</sub> target
VA	X	-0.83 ( $p < 0.01$ )	-0.52 ( $p < 0.01$ )	-0.60 ( $p < 0.01$ )	-0.62 ( $p < 0.01$ )	X	-0.80 ( $p < 0.01$ )	-0.62 ( $p < 0.01$ )	-0.55 ( $p < 0.01$ )	-0.63 ( $p < 0.01$ )
M		X	+0.57 ( $p < 0.01$ )	+0.38 ( $p < 0.05$ )	+0.42 ( $p < 0.02$ )		X	+0.59 ( $p < 0.01$ )	+0.43 ( $p < 0.02$ )	+0.62 ( $p < 0.01$ )
H			X	+0.08 ( $p > 0.1$ )	+0.27 ( $p > 0.1$ )			X	+0.31 ( $p < 0.1$ )	+0.39 ( $p < 0.05$ )
GR <sub>Red</sub> target				X	+0.83 ( $p < 0.01$ )				X	+0.92 ( $p < 0.01$ )
GR <sub>Green</sub> target					X					X

Note: \* Number of eyes examined 34; VA-visual acuity; M,H-characteristics of image analysis; GR Red/Green targets-characteristics of glare disability test at red and green targets.

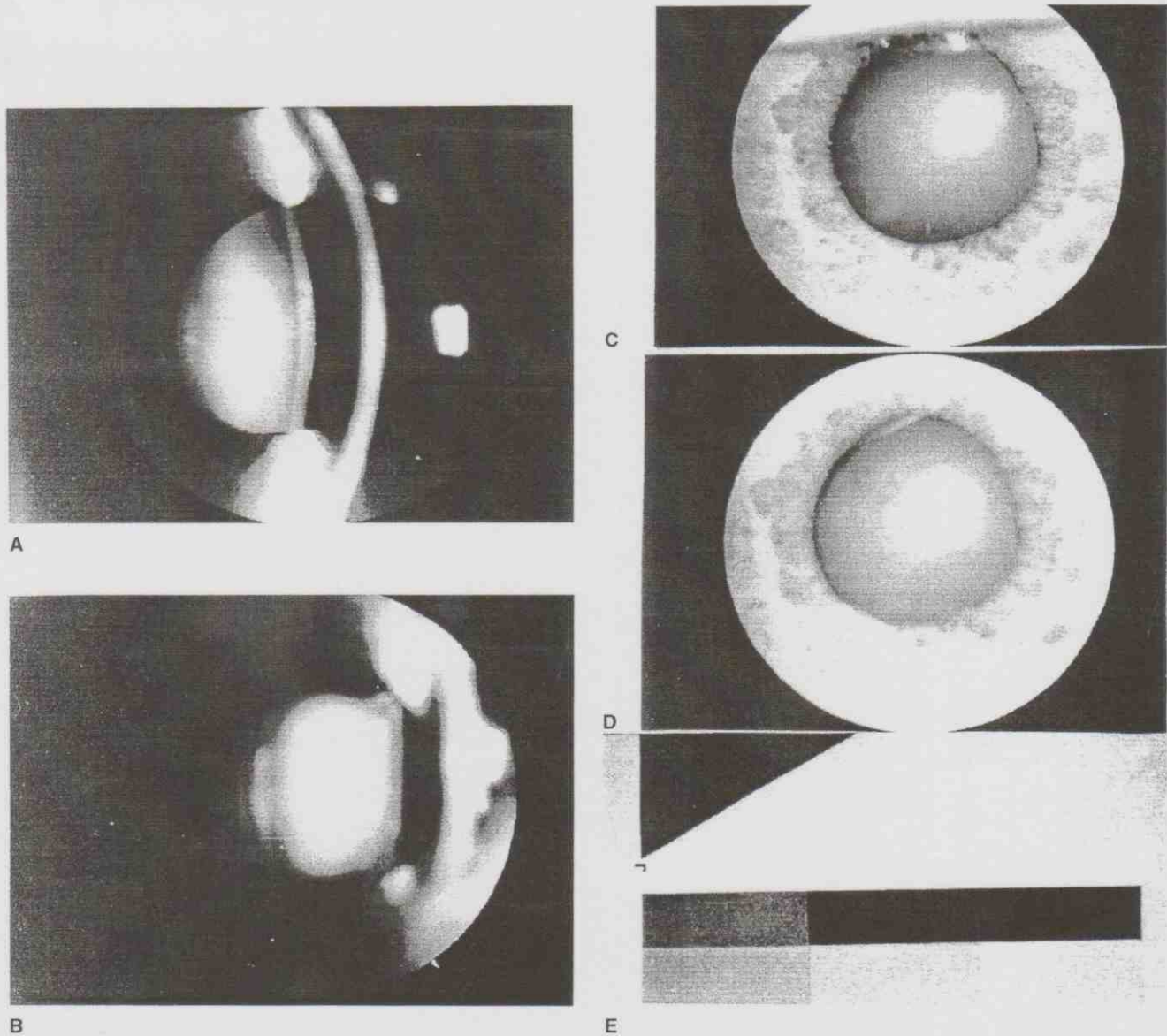


Fig. 5. Images of a human lens with a senile cataract (cortico-nuclear opacities, grade 4, age 75 years, F). (A), (B). The subsequent slit images in optical section documenting in the focal plane: (A) light scattering in the anterior subcapsular, anterior cortical and nuclear regions of the lens; (B) marked light scattering in the nucleus and posterior cortical region outlined by the lens optical scanning with the focal plane movement inside the lens thickness. (C), (D) Retro-illumination lens images with a focal plane positioned (C) onto the iris and (D) on the posterior lens layers. Opacities in the cortical layers are demonstrated as the white background inclusions in the boundary of the pupil locally masked by the flash light output. (E) The neutral density step reference wedge captured in the plane of the camera focus and allowing correction for variations in film development and flash light output.

(right or left), image analytical characteristic (M and H), and glare radius (at red and green targets).

All correlation coefficients for the image analytical characteristics were between 0.554 ( $p < 0.05$ ) and 0.953 ( $p < 0.01$ ). The glare test values of correlation coefficients approached 0.998 ( $p < 0.01$ ). Overall, the reproducibility for one operator was good. The grand average of correlation values for the image analytical characteristics is 0.830 and 0.998, correspondingly, for the glare test readings. Since the difference between the 2 visits was small, the intra-operator results were averaged and the mean, between subject variance, and extra variance from repeated readings were computed (Table 3).

Figs. 7 and 8 and Table 4 summarize the clinical effects of NAC treatment (Group II) monitored by VA, glare sensitivity and image analytical measurements over 6 months in relation to baseline (Trial 1) and follow up over 24 months using VA, photoslit-lamp and image analytical assessment (Trial 2). In control Group I the comparison with the baseline study showed some variability in densitometric readings, gradual negative advance in glare sensitivity and almost the lack of VA changes over 6 months. A slow decrease in VA and increase of image analytical characteristics were observed over 24 months compared to the baseline at enrollment. Glare sensitivity indicated changes in lens clarity when densitometric readings obtained at 5–6-

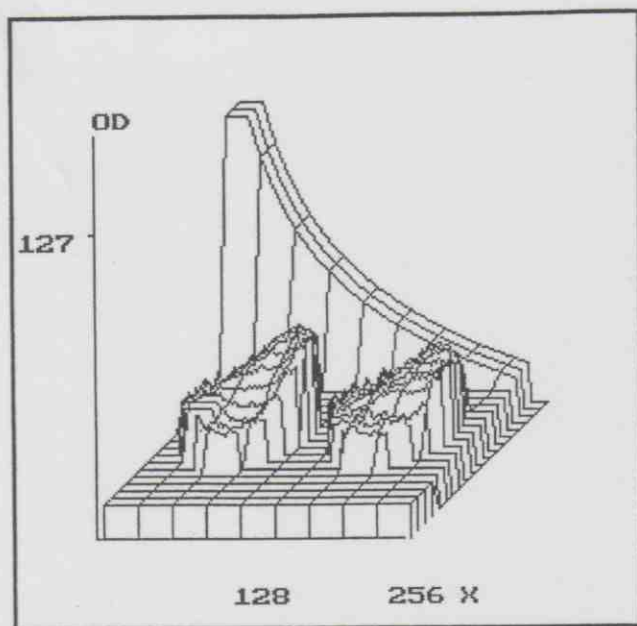


Fig. 6. Image analysis of the lens with cataract (lens opacities in cortical and nuclear regions, grade 1–2, age 66 years, F) under the effect of 4-months-treatment with 1% N-acetylcarnosine. 3-D computer graphics represents opacities in the lens layers reconstructed from subsequent slit-lamp images and analytical processing. The image functions and quantitation are coevaluated to the linear scale of the optical wedge. Ordinate (y-axis): 0–200 gray levels (optical density: 0.0–2.0 units); abscissa (x-axis): number of characteristic linear densitometric pixels, 0–255; applicate (z-axis), antero-posterior direction: number of lens morphological layers from anterior cortex through the nucleus to the posterior cortical layers (1–10). Left image: baseline status of the lens; right image: 4-months of treatment with instillations of 1% N-acetylcarnosine. Significant ( $p < 0.01$ ) partial decrease in optical density (opacity) is seen in posterior cortical layers of the examined lens. The displayed densitograms are means ( $SD \leq 3\%$ ) of the normalized data in each pixel. Each condition of measurement was repeated four times.

month follow-up examination did not differ significantly with baseline (Fig. 7). By the 5–6-month interval the significant improvement in lens clarity was found in 17 out of 41 eyes treated with NAC (Trials 1 and 2) as documented by significant decrease of M and H characteristics during im-

age grading. By the same follow-up interval, gradual improvement in VA to 7–100% concomitantly occurred in 37 out of the 41 treated eyes with NAC and the significant improvement of glare sensitivity at red and green targets to 27–100% was shown in 16 out of the 18 eyes treated with NAC (Table 4, Group II).

The NAC-treated eyes had statistically significant differences in VA, glare sensitivity and characteristics of image analysis from the control Group I ( $p < 0.001$ ) at the 6-month examination interval as shown by the overall t-test results in relation to the baseline values. 3-D computer graphics showed a cataract lens treated with NAC for 4 months in relation to the baseline image as displayed by the spatial technique and coevaluated with the optical wedge scale (Fig. 6). The digitized constitution of the opacities demonstrates a smooth significant decrease of optical heterogeneities in the lens posterior cortical region upon the application of NAC. Layer-by-layer computerized analysis of the lens opacities permitting the proportional assignment of illumination intensities in the image pixels documented the real changes in opacity densities during the topographic assembling independent to an increased masking of the deeper lens layers by an apparent increase in opacity of the middle layers.

The data obtained by the same observer in Trial 2 illustrate examinations over 24 months of the 23 eyes treated with NAC to show the alleged effect of the treatment sustainable over more prolonged periods (Table 4, Figs. 8, 9). In Group 2, 20 out of the 23 examined eyes ranged with a 12–67% improvement in acuity remaining stationary in 3 cases by the 24-month follow-up interval. Image analytical characteristics showed the significant improvement to 11–49% in 11 out of the 23 treated eyes with NAC and 12 stationary cases during such treatment over 24 months. In 41 eyes with different localization and grade of cataract, the prolonged treatment with NAC did not seem to result in a worsening of the final 24-month visual outcome. The overall clinical results observed in the NAC-treated Group II by the 24-month period of examination significantly differed ( $p < 0.001$ ) from the control Group I (Table 4) in the eyes with cortical, posterior subcapsular, nuclear or

Table 3  
Summary statistics for intra-operator correlation

Eye Right/Left	Number of eyes examined	Image analytical/ Glare test characteristic	Mean	Between V.	Extra V.	Correlation
Right	19	M	0.450	0.070	0.021	0.953*
Left	15	M	0.460	0.061	0.024	0.943*
Right	19	H	137	40	30	0.869*
Left	15	H	150	20	32	0.554**
Right	19	GR red target	22	15	1	0.998*
Left	14	GR red target	18	11	1	0.997*
Right	18	GR green target	21	15	1	0.999*
Left	14	GR green target	19	9	1	0.997*

\*  $p < 0.01$ , \*\*  $p < 0.05$ . The statistical values of measurements were computed from two visits of twenty patients (baseline study).

